Vol. 12, No. 2 (2026), pp.37–45

Journal of Multidisciplinary Research in Healthcare

Diagnostic Accuracy of 3D USG versus Hysterosalpingography Using MRI as Reference Standard for Müllerian Duct Anomalies

Revati Tekwani[1*] and Hemangini Thakkar[1]

[1]*Department of Radiology, Seth GS Medical College and KEM Hospital, Mumbai, India.*

[*]tekwanirevati6@gmail.com (Corresponding Author)

RESEARCH ARTICLE **Open Access**

ARTICLE INFORMATION

Received: April 02, 2026
Accepted: June 08, 2026
Published Online: July 05, 2026

Keywords:
Müllerian duct anomalies, 3D ultrasonography, Hysterosalpingography, Infertility

DOI: 10.15415/jmrh.2026.122003

ABSTRACT

Background: Müllerian duct anomalies (MDAs) significantly contribute to infertility and lead to poor reproductive outcomes. However, MDAs are usually underdiagnosed. It is important to make an appropriate diagnosis of MDAs to treat infertility. Magnetic resonance imaging (MRI) is the gold standard for the diagnosis of MDAs. However, three-dimensional ultrasonography (3D USG) has become a promising diagnosis method for MDAs.

Purpose: The aim of the present study was to analyze the diagnostic accuracy of 3D USG in the diagnosis of MDAs.

Methods: A cross-sectional study was conducted in a tertiary care teaching hospital over 18 months. A total of 30 patients with suspected MDAs were included in the study. All patients underwent hysterosalpingography (HSG), 3D USG, and MRI. The diagnostic performance of HSG and 3D USG was evaluated. Agreement between different modalities was also analyzed.

Results: The most common anomalies were septate and subseptate uteruses, followed by arcuate, didelphys, and unicornuate uteruses. 3D USG demonstrated 100% sensitivity, specificity, PPV, NPV, and diagnostic accuracy, with perfect agreement with MRI (kappa = 1.00). HSG showed a sensitivity of 63.33% and an accuracy of 61.29%, with 8.33% NPV and moderate agreement with MRI (kappa = 0.51). HSG usually misclassified a septate uterus as bicornuate and failed to detect certain anomalies such as an accessory cavitated uterine mass.

Conclusion: 3D ultrasonography is a highly accurate, reliable, and non-invasive technique for diagnosing MDAs. It may serve as a first-line imaging tool, whereas HSG has limited diagnostic utility.

1. Introduction

Infertility is defined as the inability to conceive after one year of regular unprotected intercourse. However, in women of advanced reproductive age (>35 years), infertility evaluation is recommended after six months of unsuccessful pregnancy (Jacobson *et al.*, 2018). Standardized guidelines for the assessment of infertility have been prescribed by the Practice Committee of the American Society for Reproductive Medicine (ASRM). Despite comprehensive evaluation, approximately 15–30% of infertile couples are diagnosed with unexplained infertility (Quaas & Dokras, 2008). Among the various etiologies, Müllerian duct anomalies (MDAs) represent a clinically significant cause of infertility. MDAs are associated with adverse reproductive outcomes, including infertility, recurrent first-trimester abortions, preterm labor, and retained placenta (Chandler *et al.*, 2009). MDAs arise due to abnormal development of the paramesonephric (Müllerian) ducts during embryogenesis. The prevalence of MDAs ranging from 0.001% to 10% in the general population and up to 8–10% in women with poor reproductive outcomes. Notably, due to the close embryological relationship between the genital and urinary systems, associated renal anomalies may be present in up to 25% of affected individuals (Ribeiro *et al.*, 2009).

The Müllerian ducts give rise to the fallopian tubes, uterus, cervix, and the upper two-thirds of the vagina, while the ovaries and lower one-third of the vagina develop from the primitive yolk sac and sinovaginal bulb, respectively (Chandler *et al.*, 2009). Normal development of the Müllerian system occurs in three sequential phases: organogenesis, fusion, and septal resorption. Disruptions of development at different stages lead to specific anomalies. Failure of organogenesis results in uterine agenesis, hypoplasia, or a unicornuate uterus. Failure of fusion leads to a bicornuate or didelphys uterus. The defects in septal resorption result in a septate or arcuate uterus (Bhamidipaty-Pelosi *et al.*, 2024). It is important to accurately classify MDAs because they have different clinical effects and management strategies. The ASRM classification system is the most popular system to classify the MDAs. It is important to note that certain MDAs do not fit into the standard diagnostic categories, and, therefore, detailed morphological examination is essential in atypical cases rather than imposed classification (Dykes *et al.*, 2007).

Hysterosalpingography (HSG) has traditionally been used during infertility evaluation because it provides information regarding uterine cavity morphology and tubal patency. However, HSG has limitations in evaluating the external uterine contour and may incorrectly differentiate between septate and bicornuate uteri (Schankath *et al.*, 2012). Various imaging modalities play an important role in the assessment and classification of MDAs. Invasive procedures like hysteroscopy and laparoscopy are performed only when the imaging modalities fail to provide sufficient information on MDAs. The first choice of diagnosis is two-dimensional (2D) transabdominal ultrasonography (USG). It is followed by the three-dimensional (3D) USG. Magnetic resonance imaging (MRI) is the best choice for MDAs because it has better soft tissue contrast and can show images from different angles (Dixit *et al.*, 2025).

Previous studies have demonstrated high diagnostic accuracy of MRI and 3D USG in diagnosing MDAs. However, comparative data evaluating HSG and 3D USG using MRI as a reference standard remain limited, particularly in resource-limited settings. Therefore, the present study was undertaken to evaluate the diagnostic performance of these modalities (Senger *et al.*, 2017). In this context, the present study was conducted to evaluate the diagnostic accuracy and efficacy of 3D ultrasonography in comparison with HSG, using MRI as the reference standard, with the objectives of determining the prevalence of various types of Müllerian duct anomalies and assessing the concordance of findings between 3D ultrasonography, HSG, and MRI in patients with suspected Müllerian duct anomalies.

2. Material and methods

2.1. Study Design and Setting

This cross-sectional observational study was conducted in the Department of Radiology at a tertiary care teaching hospital over a period of 18 months. All patients referred with suspected MDA during the study period were included. A total of 30 cases were included in the study. A detailed clinical history was recorded prior to imaging (Figure 1).

2.2. Inclusion and Exclusion Criteria

All patients suspected to have MDA based on clinical history or examination and advised to undergo USG, HSG, and MRI were included. For HSG, patients who were pregnant (uterine or ectopic), had undergone prior surgical correction of Müllerian anomalies, had active genital tuberculosis or infection, hypersensitivity to contrast agents, active vaginal bleeding, or suspected malignancy were excluded. For MRI, exclusion criteria included the presence of implanted pacemakers or defibrillators, ferromagnetic aneurysm clips, cochlear implants, certain ocular implants, and metallic foreign bodies.

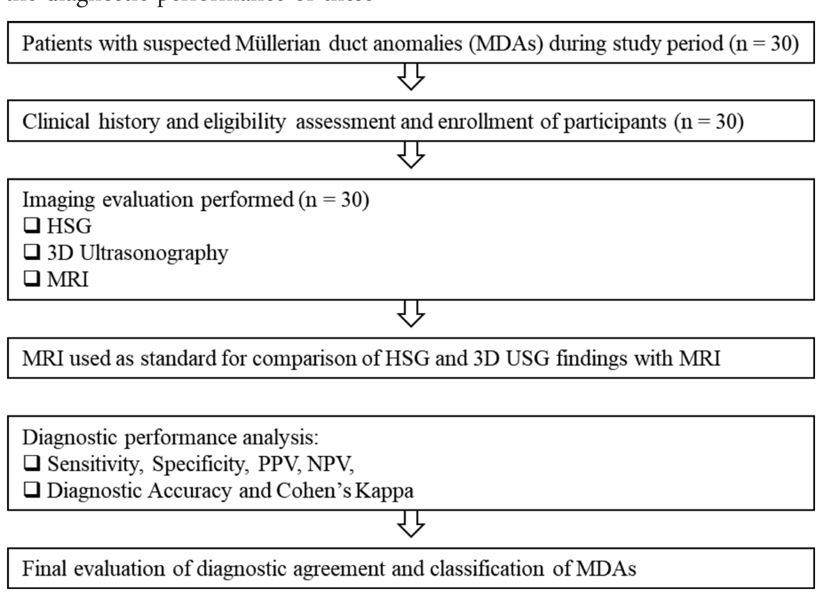

Figure 1: Study Flow Diagram Showing Patient Selection, Multimodality Imaging Assessment, and Diagnostic Evaluation Process

2.3. Hysterosalpingography (HSG)

HSG was performed under fluoroscopic guidance around the 9th day of the menstrual cycle. The procedure was carried out under aseptic precautions with the patient in a lithotomy position and with a female attendant present. After cervical cannulation, contrast medium was injected, and spot images were obtained to evaluate the uterine cavity, fallopian tubes, and peritoneal spill. Imaging parameters included 80 kV and 10 mAs with a field of view of 9 inches. The procedure duration was approximately 20–25 minutes.

2.4. Ultrasonography (USG)

All patients first had 2D USG done, and then they had 3D transvaginal USG done with a 5–7 MHz curvilinear probe and a dedicated 3D volume probe. A 3D volume acquisition box was placed over the uterus, and at least two volumes were taken with a sweep angle of 90 to 120 degrees. The average time for an USG was about 10 minutes.

2.5. Magnetic Resonance Imaging (MRI)

A 1.5 Tesla scanner was used to take an MRI of the pelvis. The protocol included multiplanar T2-weighted turbo spin-echo (TSE) sequences in axial, coronal, and sagittal planes with a slice thickness of 3.5 mm, a field of view of 320 mm, a repetition time (TR) of 7300 ms, and an echo time (TE) of 101 ms. The scan took about 20 to 25 minutes in total.

2.6. Diagnostic Criteria

We used the ASRM classification system to group MDAs across all imaging types. The distinction among septate, bicornuate, and arcuate uteri was based on objective criteria and measurements prescribed by Ludwin *et al.*

2.7. Statistical Analysis

Continuous variables were expressed as mean ± standard deviation, while categorical variables were expressed as frequencies and percentages. Sensitivity, specificity, positive predictive value, negative predictive value, diagnostic accuracy, and Cohen's kappa coefficient were calculated. A p-value <0.05 was considered statistically significant.

3. Results

The study included 30 patients. The majority of patients (60.0%) were aged between 23 and 26 years, followed by 40.0% of patients aged 27 to 30 years. The mean age of the patients was 26.23 ± 1.83 years. The mean duration of marriage was 4.40 ± 1.45 years, with a range of 2 to 8 years (Table 1).

Table 1: Demographic Characteristics of Study Population (N = 30)

Parameter	Domain	Value
Age Group (years), n (%)	23–26	18 (60.0)
	27–30	12 (40.0)
Age (years)	Mean ± SD	26.23 ± 1.83
	Range	23–30
Duration of Marriage (years)	Mean ± SD	4.40 ± 1.45
	Range	2–8

The clinical profile of the study population indicates that recurrent abortions were the most common complaint (46.7%), followed by primary infertility (43.3%). Secondary infertility was less common (10.0%). Dysmenorrhea was observed in 6.7% of patients, while both galactorrhea and headache were reported in 3.3% each (Table 2).

Table 2: Clinical Profile of Patients (N = 30)

Complaint	Number of Cases	Percentage (%)
Primary infertility	13	43.3
Secondary infertility	3	10.0
Recurrent abortions	14	46.7
Dysmenorrhea	2	6.7
Galactorrhea	1	3.3
Headache	1	3.3

HSG correctly identified an arcuate (3/3, 100%) and a unicornuate uterus (1/1, 100%). A subseptate uterus was correctly diagnosed in 10/15 cases (66.7%), with misclassification as arcuate in 3/15 (18.7%) and septate in 2/15 (12.5%). A septate uterus was correctly identified in 3/7 cases (42.9%), with 4/7 (57.1%) misdiagnosed as bicornuate. Didelphys uterus was correctly diagnosed in 1/2 cases (50%), with 1/2 (50%) misclassified as unicornuate. The single ACUM case (1/1, 100%) was misdiagnosed as normal. One normal case (1/1, 100%) was misclassified as arcuate (Table 3). 3D USG correctly identified all cases of ACUM (1/1, 100%), arcuate (3/3, 100%), didelphys (2/2, 100%), septate (7/7, 100%), subseptate (15/15, 100%), unicornuate (1/1, 100%), and normal uterus (1/1, 100%), with no misclassification (Table 4).

3D USG demonstrated sensitivity, specificity, PPV, NPV, and accuracy of 100% each (95% CI: 88.43–100.0 for sensitivity; 2.50–100.0 for specificity; 88.78–100.0 for accuracy). In contrast, HSG showed sensitivity of 63.33% (95% CI: 43.86–80.07), specificity of 0.00% (95% CI: 0.00–97.50), PPV of 95.00% (95% CI: 93.54–96.15), NPV of 8.33% (95% CI: 5.37–12.70), and accuracy of 61.29% (95% CI: 42.19–78.15). (Table 5).

Table 3: Comparison of HSG Findings with MRI (Reference Standard)

MRI Diagnosis	N	Subseptate	ACUM	Arcuate	Didelphys	Septate	Unicornuate	Normal	Bicornuate
ACUM	1	–	–	–	–	–	–	1 (100)	–
Arcuate	3	–	–	3 (100)	–	–	–	–	–
Didelphys	2	–	–	–	1 (50)	–	1 (50)	–	–
Septate	7	–	–	–	–	3 (42.9)	–	–	4 (57.1)
Subseptate	15	10 (66.7)	–	3 (18.7)	–	2 (12.5)	–	–	–
Unicornuate	1	–	–	–	–	–	1 (100)	–	–
Normal	1	–	–	1 (100)	–	–	–	–	–

Table 4: Comparison of 3D USG Findings with MRI

MRI Diagnosis	N	ACUM	Arcuate	Didelphys	Septate	Subseptate	Normal	Unicornuate
ACUM	1	1 (100)	–	–	–	–	–	–
Arcuate	3	–	3 (100)	–	–	–	–	–
Didelphys	2	–	–	2 (100)	–	–	–	–
Septate	7	–	–	–	7 (100)	–	–	–
Subseptate	15	–	–	–	–	15 (100)	–	–
Unicornuate	1	–	–	–	–	–	–	1 (100)
Normal	1	–	–	–	–	–	1 (100)	–

Table 5: Diagnostic Performance of HSG and 3D USG (Using MRI as Gold Standard).

Parameter	HSG (%)	95% CI	3D USG (%)	95% CI
Sensitivity	63.33	43.86–80.07	100.0	88.43–100.0
Specificity	0.00	0.00–97.50	100.0	2.50–100.0
Positive Predictive Value	95.00	93.54–96.15	100.0	–
Negative Predictive Value	8.33	5.37–12.70	100.0	–
Accuracy	61.29	42.19–78.15	100.0	88.78–100.0

3D USG demonstrated sensitivity and PPV of 100% each (95% CI for sensitivity: 84.56–100.0). In comparison, HSG showed sensitivity of 63.64% (95% CI: 40.66–82.80) and PPV of 100% (Table 6). All septate/subseptate cases (22/22, 100%) showed EC >15 mm, with FC <10 mm in 10/22 (45.5%) and no fundal cleft in 12/22 (54.5%). All arcuate cases (3/3, 100%) showed EC >10 mm with FC <10 mm (3/3, 100%) (Table 7). HSG showed a kappa value of 0.51 indicating moderate agreement, whereas 3D USG showed a kappa value of 1.00 indicating perfect agreement with MRI (Table 8).

Table 6: Diagnostic Performance for Septate/Subseptate Uterus

Parameter	HSG (%)	95% CI	3D USG (%)	95% CI
Sensitivity	63.64	40.66–82.80	100.0	84.56–100.0
Positive Predictive Value	100.0	–	100.0	–

Table 7: Endometrial Cleft and Fundal Cleft Assessment on 3D USG

Diagnosis	N	EC >15 mm	EC >10 mm	FC <10 mm	No Fundal Cleft
Septate/Subseptate	22	22 (100)	–	10 (45.5)	12 (54.5)
Arcuate	3	–	3 (100)	3 (100)	–

Table 8: Agreement with MRI (Cohen's Kappa)

Modality	**Kappa Value**
HSG	0.51
3D USG	1.00

Multimodality imaging findings of Müllerian duct anomalies are illustrated in Figure 2. A septate uterus was demonstrated on HSG as two uterine horns with an acute intercornual angle (a), while 3D ultrasonography showed division of the endometrial cavity with preserved external fundal contour (b), and MRI confirmed the diagnosis (c). A unicornuate uterus was identified on HSG as a single banana-shaped uterine horn deviated to the right (d), which was corroborated by 3D USG (e) and MRI (f). The Didelphys uterus was visualized on HSG as two separate uterine cavities with independently cannulated cervices (g), with confirmation on 3D USG (h) and MRI (i). A normal uterine cavity with bilateral cornua and fallopian tubes was demonstrated on HSG (j) (Figure 2).

A case of ACUM was identified on 3D USG as a cavitated lesion adjacent to a normal uterine cavity (k), with MRI confirming the diagnosis (l). In another case, HSG suggested a bicornuate uterus due to widely separated uterine horns (m); however, 3D USG demonstrated a subseptate uterus with no significant external fundal cleft (n), which was subsequently confirmed on MRI (o) (Figure 2).

Associated adenomyosis was identified in cases of septate uterus, where HSG showed an irregular endometrial lining (p), 3D USG demonstrated an indistinct endomyometrial junction (q), and MRI confirmed the findings (r and t). Additional 3D USG images also demonstrated features suggestive of adenomyosis (s) (Figure 2).

An arcuate uterus was identified on HSG as a saddle-shaped endometrial indentation (u), with 3D USG showing an indentation between 10 and 15 mm (v) and MRI confirming the diagnosis (w). In contrast, mild endometrial indentation reported as arcuate uterus on HSG (x) was correctly identified as a normal variant on 3D USG with indentation <10 mm (y), which was confirmed on MRI (z) (Figure 2).

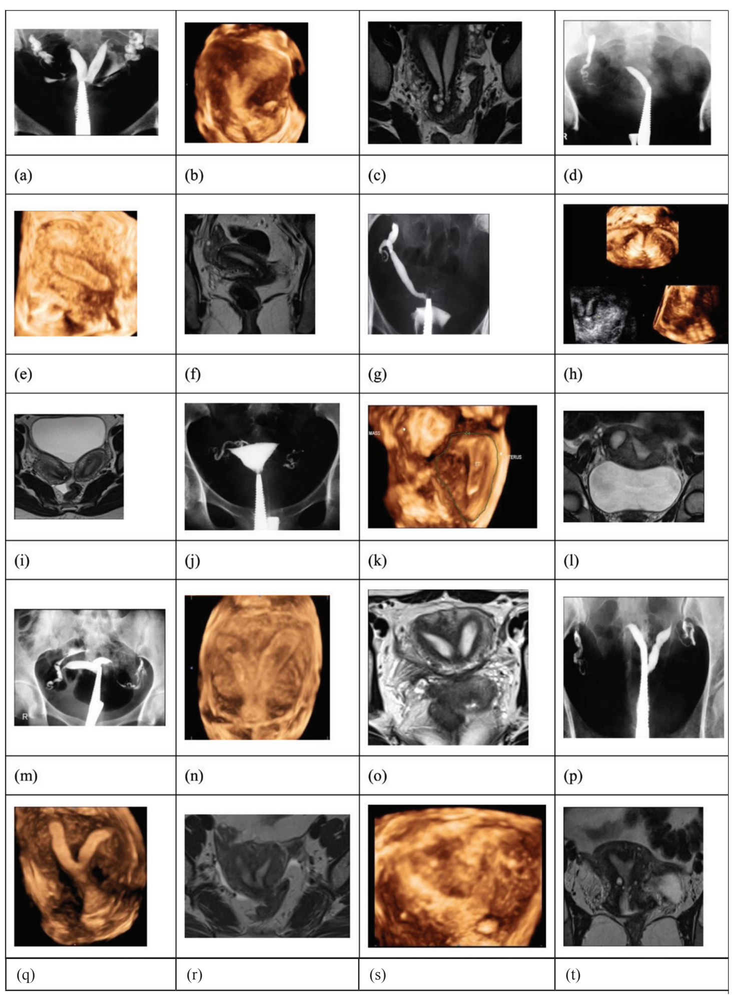

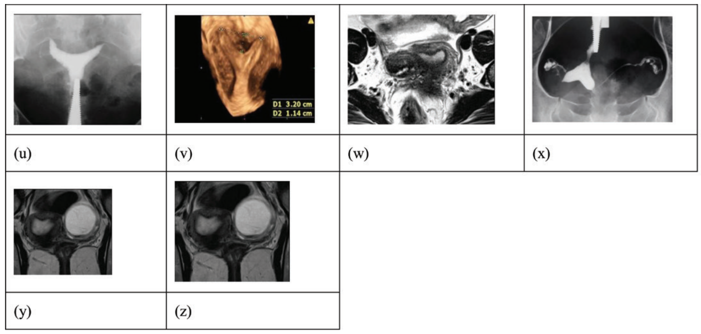

Figure 2: Multimodality Imaging Findings of Müllerian Duct Anomalies using HSG, 3D USG, and MRI

The panels demonstrate representative cases of septate uterus, subseptate uterus, bicornuate uterus (misdiagnosed on HSG), unicornuate uterus, didelphys uterus, arcuate uterus, ACUM, and normal uterine variants.

4. Discussion

During embryogenesis, Müllerian ducts fuse to form the uterus, cervix, and upper two-thirds of the vagina. The failure of this developmental process leads to the MDAs. Different classification systems have been proposed to classify the MDAs. ASRM and ESHRE-ESGE classifications are the most commonly used classification systems. ESHRE-ESGE is a more detailed classification system, as it includes complications with the uterus, cervix, and vagina. However, ESHRE-ESGE is based on the myometrial thickness, which can be different for each (D'hoore *et al.*, 2026). The ASRM classification, on the other hand, organizes the anomalies by developmental failure into descriptive categories. The ASRM classification was utilized in this study because comprehensive evaluation of myometrial thickness was not possible with 3D ultrasonography. Cases with vaginal anomalies were excluded, as these cases typically exhibit primary amenorrhea and cannot be sufficiently assessed using 3D transvaginal sonography or HSG (Dixit *et al.*, 2025).

The present study included 30 patients who were suspected to have MDAs on 3D ultrasonography, HSG, and MRI. The demographic data showed that most of the patients were in their early reproductive age, with an average age of 26.23 years and an average marriage length of 4.40 years, which shows that they had been infertile for a long time. In clinical practice, the predominant presentations were recurrent abortions (46.7%) and primary infertility (43.3%), aligning with the established correlation of MDAs with negative reproductive outcomes (Ganti *et al.*, 2024; Koya *et al.*, 2024). The current study revealed that septate and subseptate uteri were the predominant anomalies, followed by arcuate, didelphys, and unicornuate uteri and a case of ACUM. These results are in line with prior studies that indicated that a septate uterus is the most common MDA. It is also a significant factor in infertility and recurrent pregnancy loss (Deutch & Abuhamad, 2008; Grimbizis *et al.*, 2013).

In our study, HSG showed low diagnostic accuracy in distinguishing between septate and bicornuate uteri. Previous studies have noted similar limitations for HSG. The misclassification between septate and bicornuate uteruses was found to be a common diagnostic error (Pellerito *et al.*, 1992; Reuter *et al.*, 1989). Pellerito *et al.* reported that HSG is less efficient than MRI in detecting uterine abnormalities (Pellerito *et al.*, 1992). In our study, HSG accurately identified only 42.9% of septate cases. It frequently misclassified them as having a bicornuate uterus. HSG also failed to detect ACUM, likely due to its inability to assess myometrial pathology. On the other hand, 3D USG was found to have high diagnostic accuracy, matching with MRI. These results align with prior studies that have demonstrated the superior diagnostic efficacy of 3D USG. Deutch and Abuhamad showed that 3D USG gives a clear image of both the inside and outside of the uterus, which makes it easier to accurately classify abnormalities (Deutch & Abuhamad, 2008). Salim *et al.* and Bermejo *et al.* also found that 3D USG and MRI were very similar, with diagnostic accuracy that was almost as good as MRI (Bermejo *et al.*, 2010; Salim *et al.*, 2003). Jurkovic *et al.* also showed that 3D USG is better than HSG and 2D ultrasound (Jurkovic *et al.*, 1995).

The ability of 3D USG to accurately analyze both the endometrial cavity and fundal contour makes it helpful for analyzing the difference between a septate and a bicornuate uterus. In our study, all septate and subseptate uteri showed an endometrial cleft depth >15 mm. These were associated with an absent or minimal fundal cleft. In contrast, arcuate uteri showed a shallower cleft. These results align with the objective criteria established by Ludwin *et al.*, thereby reinforcing the dependability of 3D USG in morphological evaluation (Ludwin *et al.*, 2013). MRI remains the gold standard for evaluation of MDAs because of its excellent soft tissue contrast and multiplanar capability (Behr *et al.*, 2012; Saleem, 2003). But MRI costs more and is difficult to get than ultrasonography. In this situation, 3D USG is a good, cheap, and non-invasive option. Prior comparative studies have also shown that MRI and 3D USG have similar diagnostic accuracy (Deutch & Abuhamad, 2008), which backs up the results of this study.

In our study, 3D ultrasound showed perfect agreement with MRI (kappa = 1.00), but HSG only showed moderate agreement (kappa = 0.51). Earlier studies have found similar results, with 3D USG being very consistent with MRI and HSG being less reliable (Bermejo *et al.*, 2010; Salim *et al.*, 2003). Overall, the results of this study agree with what has been found in other studies. They confirm that 3D ultrasonography is a very accurate and reliable way to diagnose and classify MDAs. It may also be a good alternative to MRI in routine clinical practice, while HSG is not very useful for diagnosis. A major strength of the study was the comparative evaluation of HSG and 3D USG using MRI as the reference standard. The study also included multiple imaging modalities for comprehensive assessment. The present study had several limitations. First, the sample size was relatively small, which may limit the generalizability of the findings. Second, this was a single-center study. Larger multicenter studies with broader populations are required to validate these findings.

5. Conclusion

The current study illustrates that 3D ultrasound is a very accurate, dependable, and non-invasive method for the diagnosis and categorization of MDAs. 3D ultrasonography demonstrated excellent agreement with MRI and showed high diagnostic performance in the present study. On the other hand, HSG showed low diagnostic accuracy and a lot of misclassifications, especially when it came to describing the difference between a septate and a bicornuate uterus. 3D USG also gave useful information about related conditions like adenomyosis. 3D USG is a good first-line imaging tool because it is easy to get, cheap, and very good at diagnosing problems. MRI should only be used for complicated or unclear cases.

Acknowledgement

The authors would like to thank the Department of Radiodiagnosis, Seth GS Medical College and KEM Hospital, Mumbai, and all the study participants for their cooperation and support during the conduct of this study.

Authorship Contribution

All authors contributed equally to the conception, design, data acquisition, analysis, manuscript drafting, and final approval of the manuscript.

Ethical Approval

The study was approved by the Institutional Ethics Committee (IEC-II), Seth GS Medical College and KEM Hospital, Mumbai (Project No. EC/90/2018, Protocol Version 1.1; Approval Date: 7 September 2018). Written informed consent was obtained from all participants prior to their inclusion in the study.

Funding

The work in this manuscript was supported by funds provided by the host institute and the researchers themselves. Patients were not imposed with any additional financial burden due to this study.

Declarations

The authors declare that the manuscript is original, has not been published previously, and is not under consideration for publication elsewhere. All sources of information used in this study have been appropriately acknowledged and cited.

Data Availability Statement

Authors declare that the data supporting the conclusions of this study can be obtained upon request from the corresponding author, (R Takvani). The data is not publicly accessible due to information that may compromise the privacy of research participants.

Human and Animal Rights

This study involved human participants only and was conducted in accordance with the ethical standards of the Institutional Ethics Committee and the principles of the Declaration of Helsinki. No animals were involved in this study.

Figure Permission

All figures included in the manuscript are original and were created by the authors. No copyrighted material has been reproduced, and no additional permissions were required.

Conflict of Interest

The authors declare that there is no conflict of interest regarding the publication of this paper.

AI Disclosure Statement

During the preparation of this manuscript, the author(s) used AI-assisted language tools for grammar correction, language editing, readability improvement, and refinement of academic writing. After using these tools, the author(s) thoroughly reviewed, verified, and revised all AI-assisted content to ensure accuracy, originality, and scholarly integrity. The author(s) take full responsibility for the integrity and final content of the published article.

References

Behr, S. C., Courtier, J. L., & Qayyum, A. (2012). Imaging of Müllerian duct anomalies. *RadioGraphics, 32*(6), E233–E250. https://doi.org/10.1148/rg.326125515

Bermejo, C., Martínez Ten, P., Cantarero, R., Diaz, D., Pérez Pedregosa, J., Barrón, E., Labrador, E., & Ruiz López, L. (2010). Three-dimensional ultrasound in the diagnosis of Müllerian duct anomalies and concordance with magnetic resonance imaging. *Ultrasound in Obstetrics & Gynecology, 35*(5), 593–601. https://doi.org/10.1002/uog.7551

Bhamidipaty-Pelosi, S., Kyei-Barffour, I., Volpert, M., O'Neill, N., Grimshaw, A., Eriksson, L., Vash-Margita, A., & Pelosi, E. (2024). Müllerian anomalies and endometriosis: Associations and phenotypic variations. *Reproductive Biology and Endocrinology, 22*(1), 157. https://doi.org/10.1186/s12958-024-01336-1

Chandler, T., Machan, L., Cooperberg, P., Harris, A., & Chang, S. (2009). Müllerian duct anomalies: From diagnosis to intervention. *The British Journal of Radiology, 82*(984), 1034–1042. https://doi.org/10.1259/bjr/99354802

D'hoore, L., Decroos, E., De Visschere, P. J. L., Battaglia, O., & Hamerlynck, T. (2026). Comparison of different classification systems for Müllerian duct anomalies: A retrospective observational MRI study. *Medicina, 62*(3), 592. https://doi.org/10.3390/medicina62030592

Deutch, T. D., & Abuhamad, A. Z. (2008). The role of 3-dimensional ultrasonography and magnetic resonance imaging in the diagnosis of Müllerian duct anomalies: A review of the literature. *Journal of Ultrasound in Medicine, 27*(3), 413–423. https://doi.org/10.7863/jum.2008.27.3.413

Dixit, R., Duggireddy, C. S., & Pradhan, G. S. (2025). Mullerian anomalies: Revisiting imaging and classification. *Insights into Imaging, 16*(1), 40. https://doi.org/10.1186/s13244-024-01879-2

Dykes, T. M., Siegel, C., & Dodson, W. (2007). Imaging of congenital uterine anomalies: Review and self-assessment module. *American Journal of Roentgenology, 189*(3 Suppl.), S1–S10. https://doi.org/10.2214/AJR.06.0821

Ganti, S., Arogyaswamy, P., Srinivasan, J., & Aarthy Archunan, P. (2024). Maternofetal outcomes in women with congenital uterine anomalies. *Cureus, 16*(11), e73430. https://doi.org/10.7759/cureus.73430

Grimbizis, G. F., Gordts, S., Di Spiezio Sardo, A., Brucker, S., De Angelis, C., Gergolet, M., Li, T.-C., Tanos, V., Brölmann, H., & Gianaroli, L. (2013). The ESHRE/ESGE consensus on the classification of female genital tract congenital anomalies. *Human Reproduction, 28*(8), 2032–2044. https://doi.org/10.1093/humrep/det098

Jacobson, M. H., Chin, H. B., Mertens, A. C., Spencer, J. B., Fothergill, A., & Howards, P. P. (2018). "Research on infertility: Definition makes a difference" revisited. *American Journal of Epidemiology, 187*(2), 337–346. https://doi.org/10.1093/aje/kwx240

Jurkovic, D., Geipel, A., Gruboeck, K., Jauniaux, E., Natucci, M., & Campbell, S. (1995). Three-dimensional ultrasound for the assessment of uterine anatomy and detection of congenital anomalies: A comparison with hysterosalpingography and two-dimensional sonography. *Ultrasound in Obstetrics & Gynecology, 5*(4), 233–237. https://doi.org/10.1046/j.1469-0705.1995.05040233.x

Koya, S., Radhakrishnan, K., Ravikumar, S., Kaul, S., & Desai, A. (2024). Anticipating and executing off beat pregnancies in Müllerian duct anomalies: A case series. *Journal of Family & Reproductive Health, 18*(3), 200. https://doi.org/10.18502/jfrh.v18i3.16663

Ludwin, A., Pityński, K., Ludwin, I., Banas, T., & Knafel, A. (2013). Two- and three-dimensional ultrasonography and sonohysterography versus hysteroscopy with laparoscopy in the differential diagnosis of septate, bicornuate, and arcuate uteri. *Journal of Minimally Invasive Gynecology, 20*(1), 90–99. https://doi.org/10.1016/j.jmig.2012.09.011

Pellerito, J., McCarthy, S., Doyle, M., Glickman, M., & DeCherney, A. (1992). Diagnosis of uterine anomalies: Relative accuracy of MR imaging, endovaginal sonography, and hysterosalpingography. *Radiology, 183*(3), 795–800. https://doi.org/10.1148/radiology.183.3.1584936

Quaas, A., & Dokras, A. (2008). Diagnosis and treatment of unexplained infertility. *Reviews in Obstetrics and Gynecology, 1*(2), 69. https://pubmed.ncbi.nlm.nih.gov/18769664/

Reuter, K. L., Daly, D. C., & Cohen, S. M. (1989). Septate versus bicornuate uteri: Errors in imaging diagnosis. *Radiology, 172*(3), 749–752. https://doi.org/10.1148/radiology.172.3.2528160

Ribeiro, S. C., Tormena, R. A., Peterson, T. V., Gonzáles, M. d. O., Serrano, P. G., Almeida, J. A. M. d., & Baracat, E. C. (2009). Müllerian duct anomalies: Review of current management. *São Paulo Medical Journal, 127*(2), 92–96. https://doi.org/10.1590/S1516-31802009000200007

Saleem, S. N. (2003). MR imaging diagnosis of uterovaginal anomalies: Current state of the art. *RadioGraphics, 23*(5), e13. https://doi.org/10.1148/rg.e13

Salim, R., Woelfer, B., Backos, M., Regan, L., & Jurkovic, D. (2003). Reproducibility of three-dimensional ultrasound diagnosis of congenital uterine anomalies. *Ultrasound in Obstetrics & Gynecology, 21*(6), 578–582. https://doi.org/10.1002/uog.127

Schankath, A. C., Fasching, N., Urech-Ruh, C., Hohl, M. K., & Kubik-Huch, R. A. (2012). Hysterosalpingography in the workup of female infertility: Indications, technique and diagnostic findings. *Insights into Imaging, 3*(5), 475–483. https://doi.org/10.1007/s13244-012-0183-y

Senger, K. P. S., Singh, A. K., Sharma, V., Singh, A., & Ravikumar, R. (2017). Detection of Mullerian duct anomalies: Diagnostic utility of two-dimensional ultrasonography as compared to magnetic resonance imaging. *International Journal of Reproduction, Contraception, Obstetrics and Gynecology, 6*(1), 20–29. https://doi.org/10.18203/2320-1770.ijrcog20164421